

**Evidence of electron-hole symmetry breaking in poly(*p*-phenylene vinylene)**M. Baitoul,<sup>2</sup> J. Wéry,<sup>1</sup> S. Lefrant,<sup>1</sup> E. Faulques,<sup>1</sup> J-P. Buisson,<sup>1</sup> and O. Chauvet<sup>1</sup><sup>1</sup>*Laboratoire de Physique Cristalline, Institut des Matériaux Jean Rouxel, BP 32229 2 rue de la Houssinière, 44322 Nantes, Cedex 03, France*<sup>2</sup>*Laboratoire de Physique du Solide, Faculté des Sciences Dhar el mahraz, BP 1796 Atlas, 30 000 Fes, Morocco*

(Received 4 June 2003; published 12 November 2003)

We analyze the structural distortions associated with positively and negatively charged states produced upon doping poly (*p*-phenylene vinylene) (PPV). Vibrational frequencies associated with excitations in these charged states are analyzed on the basis of the valence force field and model-compound approaches. *In situ* electron paramagnetic resonance measurements confirm the coexistence of paramagnetic and diamagnetic species in segments with different lengths. Moreover, carbon-carbon bond-length deviations calculated for oppositely charged segments with four rings and three vinyl groups ( $PV_3^{2-}$  and  $PV_3^{2+}$ ) clearly differ. Our results show unambiguously that electron-hole symmetry is not maintained in doped PPV and are able to explain the difference between electron and hole intrachain mobility in PPV.

DOI: 10.1103/PhysRevB.68.195203

PACS number(s): 78.30.-j, 63.50.+x, 71.38.-k, 76.30.-v

**I. INTRODUCTION**

Poly(*p*-phenylene vinylene) (PPV) is still nowadays extensively studied due to its ability to be used in electroluminescent diodes (LEDs). Furthermore, high conductivity can be achieved upon *n*- or *p*-type doping.<sup>1-3</sup> Charged states, namely, polarons and/or bipolarons, are produced by doping or by photoexcitation. They are associated with geometric distortion produced along the polymeric chain, due to the strong coupling between electronic states and vibrational states.<sup>4</sup> In this context, band structure calculations based on the modified neglect of differential overlap (MNDO) scheme have predicted that *n*- or *p*-type doping should result in positively and negatively charged states with the same quinoid character.<sup>5</sup> However, it has already been suggested that this electron/hole symmetry may be broken, even if no experimental confirmation has yet been given.<sup>6</sup> Such a symmetry breaking has important practical interest for which electrons and holes are injected on the polymer backbone for polymers involved in LEDs. A clear understanding of the accommodation of the electron or hole deformation by the polymer is thus required in order to optimize LED devices.

This is the focus of this paper to investigate experimentally and theoretically the structural relaxation in PPV associated with the polarons/bipolarons formation upon *n*- or *p*-type doping. In this work the effect of *p*-type doping was studied by means of *in situ* resonant Raman scattering (RRS) and infrared (IR) absorption of electrochemically *p*-doped PPV in association with electron paramagnetic resonance (EPR). A dynamical model based on the valence force field (VFF) methodology coupled to a model-compound approach is used in order to describe the structural relaxation induced by the *p* doping and its extension along the polymer chain. The same model is used to describe the relaxation of the *n*-doped polymer. In this case, we use Raman spectra obtained earlier in our group on chemically *n*-doped PPV.<sup>7</sup> Our results suggest that *n*-type doping result in a much weaker structural relaxation of the polymer than *p*-type doping. It shows that, indeed, the electron-hole symmetry is broken in this compound.

**II. EXPERIMENT**

Thin film of tetrahydrothiophenium precursor<sup>8</sup> were deposited on platinum electrode and thermally converted under vacuum ( $10^{-6}$  Torr) to obtain the conjugated PPV. A specific electrochemical cell and tetrabutylammonium tetrafluoroborate (TBABF<sub>4</sub>/ACN) (0.2 M) solution were used for the *p*-type doping experiments. Raman scattering using the 676.4-nm and 1064-nm laser lines was obtained *in situ* (during electrochemical doping) at a given potential and under equilibrium conditions. Infrared absorption spectra were recorded *ex situ*. EPR has been carried out *in situ* at different potentials in a home made cell. A small signal at  $g=2$  coming from the cell is used to calibrate the quality factor of the cavity.

The evolution of the Raman spectra as a function of the electrochemical potential are presented elsewhere.<sup>9</sup> This previous work showed that a broad oxidation wave develops between 1 V/Ag/Ag<sup>+</sup> and 1.35 V/Ag/Ag<sup>+</sup> in our experimental conditions. *In situ* optical absorption have shown that this oxidation state is associated with the onset of two absorption bands in the optical spectrum located close to 2 eV (640 nm) and 0.8 eV (1340 nm). Indeed, the onset of these two absorption bands leads us to suggest that the charge transfer occurring in the oxidation process is associated with the formation of bipolarons (Ref. 9).

**III. RESULTS AND DISCUSSION**

In the present paper, we will focus on the Raman spectra obtained at high potential (1.3 V/Ag/Ag<sup>+</sup>), close to the maximum of oxidation. Figure 1 shows that at the same oxidation potential, the frequencies and intensities of the Raman bands depend strongly on the excitation wavelength indicating thus a resonance behavior. The Raman spectrum recorded with  $\lambda_{exc}=676.4$  nm shows bands located at 1605, 1568, 1523, 1330, 1296, 1280, 1178, and 1147 cm<sup>-1</sup> [Fig. 1(b)]. Most of these bands are downshifted in frequency with respect to the Raman bands of PPV [Fig. 1(a)]. It is clear that most of the Raman band frequencies recorded with the 1064

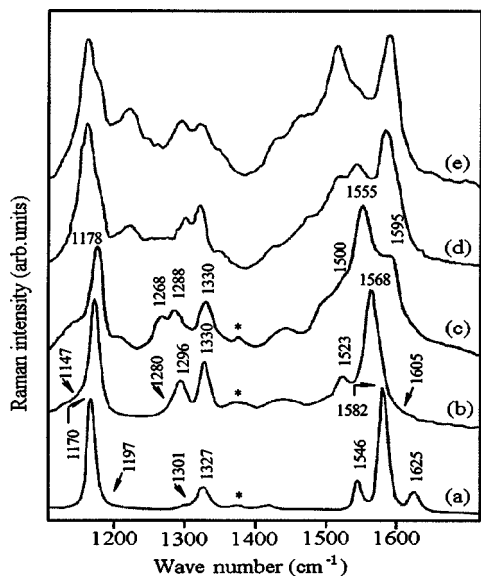


FIG. 1. Raman spectrum recorded for neutral PPV (0 V/Ag/Ag<sup>+</sup>) (a) BF<sub>4</sub><sup>-</sup> doped PPV spectra recorded at (1.3 V/Ag/Ag<sup>+</sup>) with (b) 676.4-nm and (c) 1064-nm excitation wavelengths, respectively and doped PPV-Na at maximum doping level with (d) 676.4-nm and (e) 1064-nm excitation wavelengths, respectively. The asterisk (\*) indicates the bands due to the solvent.

nm excitation [Fig. 1(c)] are more strongly downshifted when compared to those observed with the 676.4-nm excitation. Moreover one observes that Raman frequencies are in general more shifted than those obtained with Na-doped films<sup>7</sup> [Figs. 1(d) and 1(e)]. Our *in situ* RRS spectra are similar to those presented by Sakamoto *et al.*<sup>10</sup> for soluble model compounds oxidized into radical cation and dication with excitations, respectively, at 676.4 and 1064 nm. The strong analogy with the Raman spectra presented by these authors in this previous work suggests that the bands obtained with the 676.4-nm laser line are associated with polarons corresponding to the electronic transition energy at  $\sim 2$  eV. Additionally, the bands recorded with the 1064-nm laser line can be ascribed to bipolarons for which the maximum absorption is at  $\sim 0.8$  eV. These studies performed on electrochemically *p*-doped PPV put unambiguously in evidence the structural modifications upon doping which are illustrated by the frequency shifts of some Raman bands. Indeed, we observe that the downshift of the main Raman bands increases upon doping and appears stronger in the case of *p*-doped PPV. In other terms, the quinoid-character structure is more intensified when doping increases especially in the case of the *p*-doped PPV. This attests of the non-symmetry of the *p*- or *n*-type polarons/bipolarons. In Fig. 2, the infrared absorption spectrum displays doping induced bands superimposed to those of neutral PPV and to those coming from the counter-ion. Bands relative to the counter-ion are located at 1083 and 520 cm<sup>-1</sup> (Ref. 11) and the new bands induced by electrochemical doping are found at 881, 1150, 1284, and 1490 cm<sup>-1</sup>. These additional bands, similar to those generally obtained by chemical *p*-type doping or by photoexcitation, are independent of the doping nature. The appearance of these new bands has generally been correlated

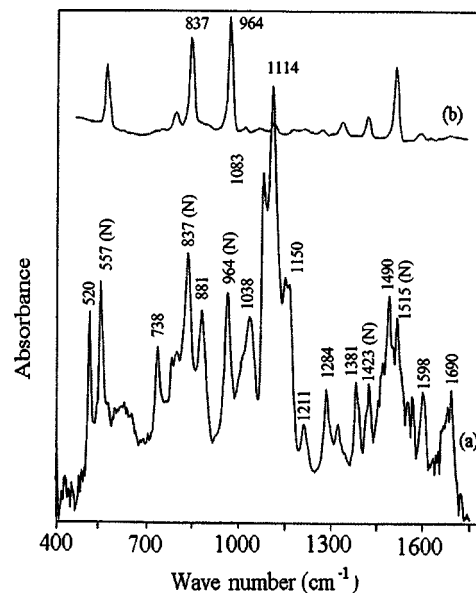


FIG. 2. Infrared spectra recorded for neutral PPV (a) and *ex situ* for BF<sub>4</sub><sup>-</sup> doped PPV (b) bands denoted with (N) originate from neutral segments.

to the presence of bipolarons. In a previous study, we have shown that the vibrational modes associated with the charged states induced by *p*-type doping are independent of the doping nature, whatever the doping method and the conversion conditions.<sup>12</sup>

In order to elucidate the nature of the charged states in *p*-doped PPV, *in situ* EPR has been performed. Figure 3 shows the evolution of the spin density against the oxidation potential  $U$ . The cycle is reversible if  $U$  does not exceed 1.5 V/Ag/Ag<sup>+</sup> beyond which overoxidation occurs.<sup>13</sup> At 0 V/Ag/Ag<sup>+</sup>, the film is EPR silent within our experimental conditions. Increasing the oxidation potential, the spin density start to increase at  $U = 1$  V/Ag/Ag<sup>+</sup>, i.e., at the onset of the oxidation wave observed in the cyclovoltammogram, but it remains very small (lower than 0.25/1000 monomers). Even at the beginning of the oxidation process, the spin to

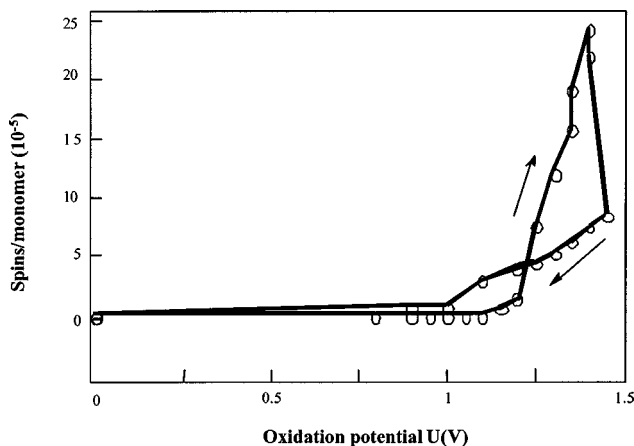


FIG. 3. Number of spins/monomer against potential  $U$  (V/Ag/Ag<sup>+</sup>) for PPV, EPR cycle recorded in TBABF<sub>4</sub>/ACN solution (0.2 M) (*in situ* static measurement).

charge ratio (not shown here) remains much lower than one (0.2% at the maximum), contrarily to polypyrrole or polythiophene for which this ratio is of the order of one in similar conditions.<sup>14</sup> This indicates that even at the beginning of the oxidation process, most of the charges recombine in diamagnetic or spineless stable species, i.e., in bipolarons. A rapid recombination of polarons into bipolarons has already been proposed in the case of doped PPV oligomers or typically *p*-doped PPV.<sup>15</sup>

Still, a small amount of polarons (spins) is detected above  $U = 1.1$  V/Ag/Ag<sup>+</sup> with a maximum density of 0.25/1000 monomers at  $U = 1.3$  V/Ag/Ag<sup>+</sup>. Indeed, we have checked that these spins are obtained in a steady state. Obviously such a small spin density confirms that most of the charges are forming bipolarons. However, the presence of the unpaired polarons deserves a comment. We suggest that these polarons are those which have been created on short segments. The coexistence of short and long segments associated with different conjugation lengths is well known in the same PPV sample.<sup>16,17</sup> Charges injected on long segments may happily condense into bipolarons because the longitudinal transfer integral is large and the Coulomb interactions are efficiently screened. This is not the case for charges injected on short segments and two possible reasons may explain the "stability" of the polarons created on short segments that (i) these polarons are "transverse" polarons, stabilized by a partial counter-ion transfer as suggested in recent theoretical studies; and<sup>18-20</sup> (ii) a second possible reason is that the Coulomb interactions, which prohibit the formation of the bipolarons, are barely screened in short segments. This latter analysis is in agreement with that of Chen *et al.*<sup>21</sup> who have shown that preferential production of bipolarons increases in oxidized polyenes when the conjugation length increases. At high potential (1.3 V/Ag/Ag<sup>+</sup>), the spin density decreases in static measurements which suggests that there is a second combination of intrachain and/or interchain polaron pairs into bipolarons on short segments.

In order to validate these experimental results, we present here an extensive assignment of the in-plane vibrational modes associated to these charged states. In particular we focus on the Ag modes, which are strongly coupled to the  $\pi$ -electron system. The calculation method is the same as previously reported.<sup>22</sup> The valence force field (VFF) was constructed by adopting that reported for benzene and PPV.<sup>7</sup> The carbon-carbon stretching force constants were adjusted phenomenologically from the linear dependence of the force constants against the doubly-squared inverse of the bond length ( $F\alpha 1/r^4$ ) established on a series of aromatic conjugated compounds.<sup>23</sup> All the compounds belong to the  $C_{2h}$  point group symmetry. The nomenclature of internal coordinates and the choice of the molecular axes are shown in Fig. 4. The geometric parameters are extracted from semi-empirical geometry optimizations<sup>24</sup> and are independent of the oligomer length. The polymer chain is considered as planar and only in-plane modes are taken into consideration. The Raman and infrared active in plane modes in the frequency range  $\leq 2000$  cm<sup>-1</sup> are  $11A_g + 9B_u$ . We focus mainly on the force constants associated with carbon-carbon bonds, which are  $F_t^2$  and  $F_{t'}^2$  for the ring and  $F_D^2$  and  $F_R^2$  for

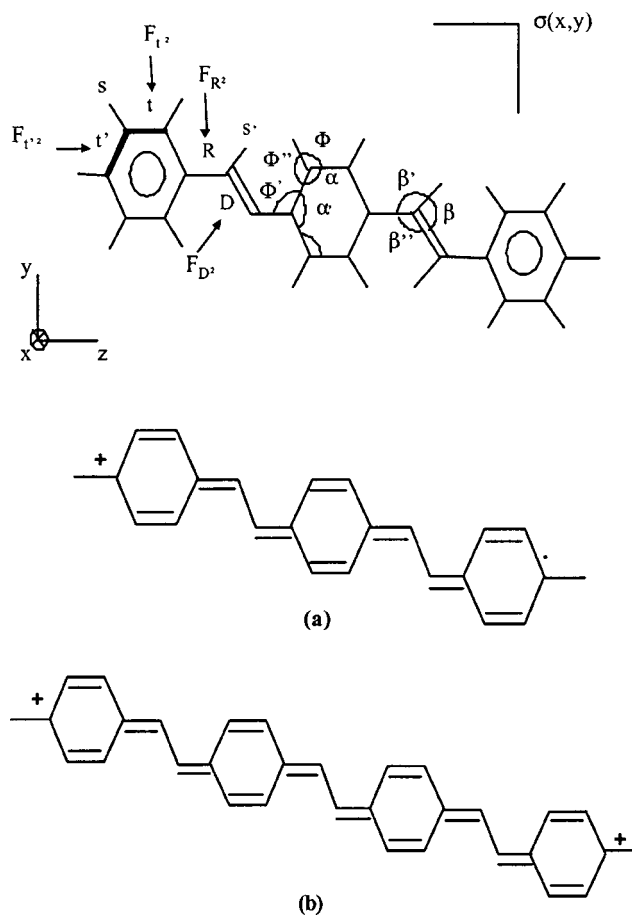


FIG. 4. Molecular axes and nomenclature of internal coordinates; geometric parameters used for the different compounds are  $t = t' = 1.40$  Å,  $s = s' = 1.06$  Å,  $R = 1.45$  Å,  $D = 1.35$  Å,  $\alpha = \alpha' = 120^\circ$ ,  $\phi = \phi' = 120^\circ$ ,  $\beta = 126^\circ$ ,  $\beta' = 114^\circ$ , and  $\beta'' = 120^\circ$ . (a)  $PV_2^{2+}$  and (b)  $PV_3^{2+}$

the vinyl group. As there is mixed contribution of the rings and the vinyl group due to coupling, it has been necessary to determine the relative Potential Energy Distribution (PED) (Ref. 7) for each vibrational mode (Table I). We can thus detail more precisely the vibrational modes by the analysis of their displacement eigenvectors and PED percentages. In this paper we present only the PED. The vibrational modes assignments of neutral PPV have been obtained with  $F_t^2 = 6.21$  mdyn/Å,  $F_{t'}^2 = 6.18$  mdyn/Å,  $F_R^2 = 5.15$  mdyn/Å, and  $F_D^2 = 7.23$  mdyn/Å.<sup>7</sup> The optimization process leads to the same set of force constants for PPV and related model compounds.

In doped PPV frequencies observed with different excitation wavelengths (676.4 and 1064 nm (Fig. 1)) have been recently assigned to polaronic and bipolaronic segments, respectively.<sup>11</sup> Some bands are independent on the excitation wavelength and have been considered to be induced by those two species. In addition, the infrared spectrum displays doping induced bands superimposed to those of neutral PPV and to those coming from the counterion (Fig. 2). We attempted to assign the IR bands observed at 1490 and 1150 cm<sup>-1</sup> to the Raman species enhanced with the 676.4-nm excitation wavelength and an iterative process finally confirmed these

TABLE I. Assignment of experimental frequencies, ( $\text{cm}^{-1}$ ), obtained with 676.4- and 1064-nm excitation wavelengths. Frequencies are calculated on  $\text{PV}_2^{+\cdot}$  and  $\text{PV}_3^{2+}$  respectively. PED\* represents main contributions relative to the CC stretching. Obs. freq. and Calc. freq. indicate the observed and calculated frequencies.

Neutral PPV		Doped PPV				Assignment PED*
676.4 nm Obs. freq.	Assignment PED*	676.4 nm Model: $\text{PV}_2^{+\cdot}$		1064 nm Model: $\text{PV}_3^{2+}$		
		Obs. freq.	Calc. freq.	Obs. freq.	Calc. freq.	
Ag: 1625	$F_D^2, F_t^2$	1605	1613	1595	1603	$F_t^2, F_{t'}^2$
1582	$F_t^2, F_{t'}^2$	1568	1566	1555	1550	$F_R^2, F_D^2$
1546	$F_{t'}^2$	1523	1522	1500	1502	$F_{t'}^2$
1327	$F_D^2$	1330	1323	1330	1314	$F_R^2$
1301	$F_D^2$	1296	1304	1288	1280	$F_R^2$
1197	$F_R^2$	1280	1277	1268	1269	$F_R^2$
1170	$F_t^2, F_R^2$	1178	1174	1178	1176	$F_t^2$
		1147	1148	1142	1149	$F_{t'}^2$
889	$F_{t'}^2$	887	887	887	890	$F_{t'}^2$
Bu: 1519		1490	1490			$F_{t'}^2$
1109		1150	1149			$F_{t'}^2$

assignments. Raman spectra indicate clearly a loss of translation symmetry on the polymer chain owing to the number of frequencies observed. For the localization of geometrical relaxation in charged states, we considered the substituted charged oligomers.<sup>10</sup> In the polaron model, the structural relaxation around the radical cation is allowed to extend on three rings and two-vinyl group labeled  $\text{PV}_2^{+\cdot}$  [Fig. 4(a)]. In the case of a bipolaron model, we consider that it extends on segments containing four rings and three vinyl groups denoted  $\text{PV}_3^{2+}$  [Fig. 4(b)]. We thus assume that short-range, intramolecular Coulomb interactions are negligible on this extension. Indeed, the stability of these species on segments containing four and five rings has been suggested in other works.<sup>10</sup>

In the modeling of the vibrational spectra of the PPV in the doped state, we have considered that the perturbation of the electronic density by the dopant induces locally a change of alternation. We have therefore modified only the force constants corresponding to carbon-carbon bonds which are the most susceptible to be disturbed. Assuming the presence of quinoid rings necessitates uncoupling interactions between carbon-carbon bonds inside the rings since  $t$  and  $t'$  now become different. We have then considered the existence of short and long charged segments such as in PPV,  $\text{PV}_2^{+\cdot}$  and  $\text{PV}_3^{2+}$  with a quinoid character structure. The force constants have been modified on the basis of an assignment of the new RRS and IR bands. We consider that the symmetry group  $C_{2h}$  is preserved for the charged segments. The force constants variations are in favor of a transition towards a quinoid character structure which is similar, for the polaron model, to that observed in the case of  $\text{FeCl}_3$ -doped PPV.<sup>25</sup> From the analysis of the carbon-carbon bond vibrations, one notices that the new band observed at  $1568 \text{ cm}^{-1}$  and calculated at  $1566 \text{ cm}^{-1}$  is assigned without any ambiguity to the C—C stretching of the vinyl group according to the PED. The band peaked at  $1523 \text{ cm}^{-1}$  is attributed to the

ring C—C stretching. One observes a weak shoulder around  $1605 \text{ cm}^{-1}$  corresponding to that calculated at  $1613 \text{ cm}^{-1}$ . This latter line contains a strong contribution of the  $F_t^2$  force constant. We have attributed it to the ring C=C stretching in rings with a quinoid character.

In the bipolaron model, the band observed at  $1595 \text{ cm}^{-1}$  is calculated at  $1603 \text{ cm}^{-1}$  and the high PED for  $F_t^2$  in this mode confirms its assignment to a ring C=C stretching. The strongest contribution of the vinyl C—C stretching occurs for a frequency calculated at  $1550 \text{ cm}^{-1}$  and observed at  $1555 \text{ cm}^{-1}$ . The frequency calculated at  $1502 \text{ cm}^{-1}$  corresponds to the C—C stretching in quinoid rings.

In summary, one observes that the weakening of the vinyl bond translated into its contribution in a vibrational mode at more lower frequency measured at  $1568 \text{ cm}^{-1}$  for the polaronic structure and at  $1555 \text{ cm}^{-1}$  for the bipolaronic one. On the other hand, the interring contribution which in the neutral PPV, occurs in the mode located at  $1197 \text{ cm}^{-1}$ , is found for polaron modes located at  $1296$  and  $1280 \text{ cm}^{-1}$  and in modes obtained at  $1330$  and  $1288 \text{ cm}^{-1}$  for the bipolaronic structure. This indicates an increasing strengthening of the  $C_{\text{ring}}-C_{\text{vinyl}}$  bond, which corroborates thus the occurrence of a quinoid character structure. From the semi-empirical relationship  $F \propto 1/r^4$  (Ref. 23), we have estimated the structural relaxation. In Fig. 5 are shown the bond lengths deduced from our model compared to those theoretically calculated by several authors.<sup>26,27</sup> One notices that the bond lengths obtained by our model are compared to the averaged values deduced from theoretical studies. These results extracted from experimental data are in reasonable agreement, essentially for the polaron model, with theoretical approaches conducted on positively charged segments obtained by removing one or two electrons in the MNDO and the valence effective Hamiltonian models.<sup>26,27</sup> Further, in the assumption of electron-hole symmetry in conducting polymers, the same

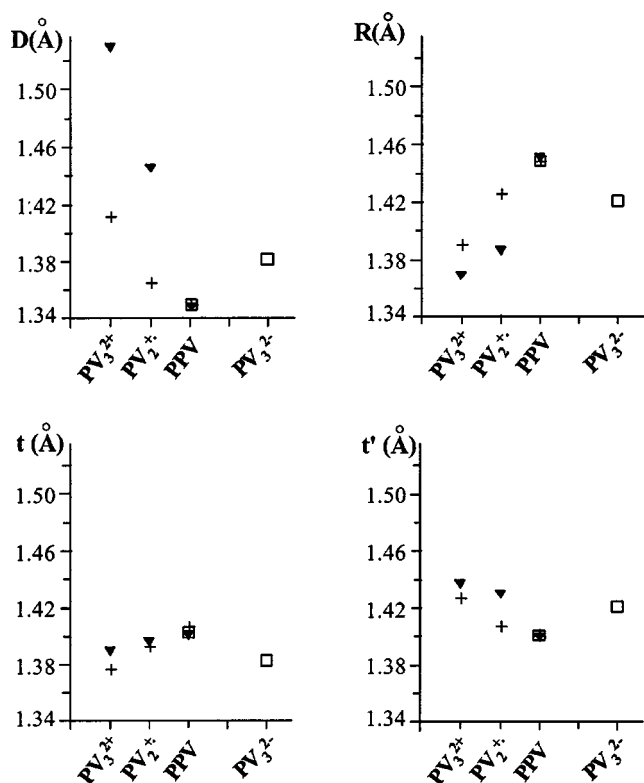


FIG. 5. Average geometry calculated by VFF for polaron and bipolaron on models:  $PV_2^{+}$  and  $PV_3^{2+}$  (▼),  $PV_3^{2-}$  (□) (Ref. 7) and by geometric optimization methods for cation and dication (+) (Ref. 27).

structural relaxation is considered for negatively charged species while the stronger deformation calculated by our model for bipolaronic segments results in greater downshifts of the vinyl CC stretching which are effectively observed in Raman spectra. The geometric distortion calculated for the

positive bipolaron evidences that the quinoid character is much more enhanced than that generally obtained with  $n$  doping<sup>7,28</sup> (Fig. 5). The weaker structural distortion that appears for the negative bipolaron is in complete agreement with the Raman frequency shifts, which never exceed 3% of the undistorted system.<sup>7</sup> These results are in agreement with those obtained by Kim *et al.*, who calculated that the effective Coulomb correlation energy associated with the negatively charged bipolarons is  $\sim 0.4$  eV greater than for positively charged ones. Consequently, there should be a severe breaking of the electron-hole symmetry in PPV contrarily to the predictions of electron-hole symmetry conservation considered in theoretical models for conjugated polymers which lead to the same relaxation for electron and hole injection on the polymer.

#### IV. CONCLUSION

The modeling of the charged states undertaken on the model compounds  $PV_2^{+}$  and  $PV_3^{2+}$  has allowed us to confirm the assignments of the experimental frequencies. We can deduce from the EPR and RRS studies that there is a coexistence of two different intrachain defects extending over three and four rings. The weak spin-to-charge ratio obtained at a low doping level indicates that polarons created on long segments rapidly combine into bipolarons and then, at more high doping level, there exists a second combination into polarons on short segments. Indeed, the polarons localized on short segments can be associated in intrachain and/or interchain polaron pairs. Positive polaronic and bipolaronic segments present a more enhanced quinoid character than negative polarons. Further, in case of hole injection in PPV, the structural relaxation difference occurring around the dopant leads to a stronger electron-vibration coupling. Therefore, these results clearly show the absence of electron-hole symmetry in this polymer.

- <sup>1</sup>J. H. Burroughes, D. D. C. Bradley, A. R. Brown, R. N. Marks, K. Mackay, R. H. Friend, P. L. Burns, and A. B. Holmes, *Nature (London)* **347**, 539 (1990).
- <sup>2</sup>C. K. Chiang, C. R. Fincher, Y. W. Park, A. J. Heeger, H. Shirakawa, E. J. Louis, and A. G. MacDiarmid, *Phys. Rev. Lett.* **39**, 1098 (1977).
- <sup>3</sup>I. Murase, T. Ohnishi, T. Noguchi, and M. Hirooka, *Synth. Met.* **17**, 639 (1987).
- <sup>4</sup>J. L. Brédas, R. R. Chance, R. Silbey, *Phys. Rev. B* **26**, 5843 (1982).
- <sup>5</sup>J.-L. Brédas, B. Themans, J. G. Fripiat, J. M. André, R. R. Chance, *Phys. Rev. B* **29**, 6761 (1984).
- <sup>6</sup>Y. H. Kim, M. J. Winokur, and F. E. Karasz, *Synth. Met.* **55–57**, 509 (1993).
- <sup>7</sup>I. Orion, J.-P. Buisson, and S. Lefrant, *Phys. Rev. B* **57**, 7050 (1998).
- <sup>8</sup>R. A. Wessling and R. G. Zimmerman, U.S. Patent No. 3,401,152 (10 September 1968).
- <sup>9</sup>M. Baïtoul, J. Wéry, S. Lefrant, J.-P. Buisson, B. Dulieu, and M.

Hamedoun, *Polymer* **41**, 6955 (2000).

- <sup>10</sup>A. Sakamoto, Y. Furukawa, and M. Tasumi, *J. Phys. Chem.* **98**, 4635 (1994).
- <sup>11</sup>C. Kvarnström, A.-S. Nyback, and A. Ivaska, *Synth. Met.* **55–57**, 503 (1993).
- <sup>12</sup>M. Baïtoul, J. Wéry, B. Dulieu, S. Lefrant, J.-P. Buisson, and M. Hamedoun, *Synth. Met.* **101**, 173 (1999).
- <sup>13</sup>M. Baïtoul, Ph.D. thesis, Fes University, 1999.
- <sup>14</sup>F. Genoud, Guglielmi, M. Nechtschein, E. Genies, and M. Salmon, *Phys. Rev. Lett.* **55**, 118 (1985).
- <sup>15</sup>C. W. Spangler and T. J. Hall, *Synth. Met.* **44**, 85 (1991).
- <sup>16</sup>J. Wéry, B. Dulieu, J. Bullot, M. Baïtoul, P. Deniard, and J.-P. Buisson, *Polymer* **40**, 519 (1999).
- <sup>17</sup>E. Mulazzi, A. Ripamonti, J. Wéry, B. Dulieu, and S. Lefrant, *Phys. Rev. B* **60**, 16 519 (1999).
- <sup>18</sup>P. Gomes Da Costa, R. G. Dandrea, E. M. Conwell, M. Fahlman, M. Logdlund, S. Stafstrom, W. R. Salaneck, S. C. Graham, R. H. Friend, P. L. Burn, and A. B. Holmes, *Synth. Met.* **55–57**, 4320 (1993).

- <sup>19</sup>P. Gomes Da Costa, R. G. Dandrea, and E. M. Conwell, *Phys. Rev. B* **47**, 1800 (1993).
- <sup>20</sup>M. N. Bussac and L. Zuppiroli, *Phys. Rev. B* **49**, 5876 (1994).
- <sup>21</sup>C. H. Cheng, J. J. Doney, G. A. Reynolds, and F. D. Saeva, *J. Org. Chem.* **48**, 2757 (1983).
- <sup>22</sup>J-P. Buisson, S. Krichène, and S. Lefrant, *Synth. Met.* **21**, 229 (1987).
- <sup>23</sup>S. Lefrant and J-P. Buisson, in *Frontiers of Polymers and Advanced Materials*, edited by P. N. Prasad (Plenum, New York, 1994).
- <sup>24</sup>O. Lhost and J-L. Brédas, *J. Chem. Phys.* **96/7**, 5279 (1992).
- <sup>25</sup>S. Lefrant, E. Perrin, J-P. Buisson, H. Eckhardt, and C. C. Han, *Synth. Met.* **29**, E91 (1989).
- <sup>26</sup>H. Eckhardt, R. H. Baughman, J-P. Buisson, S. Lefrant, C. X. Cui, and M. Kertesz, *Synth. Met.* **41–43**, 3413 (1991).
- <sup>27</sup>J. L. Brédas, D. Beljonne, Z. Shuai, and J. M. Toussaint, *Synth. Met.* **41–43**, 3743 (1991).
- <sup>28</sup>A. Simonneau, Ph.D. thesis, Nantes University, 1996.